

Coupling of shear flow and pressure gradient instabilities

I. Voronkov, R. Rankin, P. Frycz, V. T. Tikhonchuk,¹ and J. C. Samson

Department of Physics, University of Alberta, Edmonton, Alberta, Canada

Abstract. The nonlinear dynamics of a shear flow and its subsequent evolution in the equatorial plane of the inner plasma sheet is studied. A linear analysis of the ideal MHD equations reveals a hybrid vortex instability which appears because of the coupling of Kelvin-Helmholtz (KH) and Rayleigh-Taylor instabilities. The hybrid vortex mode grows faster than a KH mode, extracts ambient potential energy, and leads to vortex cells that have a larger spatial extent than a simple KH vortex. In the nonlinear stage, vortices become surge-like and may destroy the shear flow region. The relevance of this model to vortex generation and auroral arc intensifications at the inner edge of the plasma sheet is discussed.

1. Introduction

Many observations of discrete auroral arcs have shown that they are often associated with shear flow and large-scale (hundreds of kilometers) vortex structures [Steen and Collis, 1988; Elphinstone *et al.*, 1995; Samson *et al.*, 1996]. The evening and premidnight sector seems to be the most active region [Kidd and Rostoker, 1991; Murphree and Johnson, 1996; Samson *et al.*, 1996]. Some authors have suggested that vortex formation in auroral arcs might be caused by shear flows and Kelvin-Helmholtz (KH) instabilities in the auroral arc [Steen and Collis, 1988; Kidd and Rostoker, 1991; Rankin *et al.*, 1993a]. Nevertheless, we should note that KH instabilities alone do not lead to increased kinetic energy in the plasma flow and cannot explain the very large and active auroral vortices that are sometimes seen. A mechanism is needed which will allow extraction of the potential energy stored in regions of the magnetosphere, for example, the growth phase magnetosphere, in order to allow the explosive (tens of seconds) growth of the kinetic energy associated with plasma flows. A clue to what this mechanism is might be found in the fact that these active electron arcs are often seen within regions of strong $H\beta$ emissions and energetic proton (tens of keV) precipitation at the equatorward edge of the evening sector auroral region [Samson *et al.*, 1992, 1996]. These $H\beta$ emissions are on field lines which thread the inner edge of the plasma sheet in regions where there are strong earthward pressure gradients [Kistler *et al.*, 1992], particularly during substorm growth phases. Owing to the energetic ion trajectories, the strongest pressure gradients are found in the

evening sector and before local midnight [Lyons and Samson, 1992].

The strong earthward pressure gradients suggest that ballooning or Rayleigh-Taylor (RT) modes might play a role in the extraction of the potential energy stored in the near-Earth magnetotail. Nevertheless, most analyses have shown that this region is ballooning stable or only slightly unstable [Ohtani and Tamao, 1993]. Furthermore, a simple ballooning instability does not take into account the presence of the auroral arc. The presence of both shear flow in the auroral arc and strong pressure gradients in the equatorial magnetosphere suggests that a coupling of shear flow instabilities with a pressure gradient might be a possible mechanism for the formation of large-scale vortices. Viñas and Madden [1986] have already suggested that these instabilities might produce some of the ultralow frequency (ULF) magnetohydrodynamic waves seen in the Earth's magnetosphere.

It is well known that shear flows can stabilize ballooning modes with large wavenumbers [Viñas and Madden, 1986; Tajima *et al.*, 1991], in our case, large azimuthal wavenumbers. Nevertheless, the evolution of lower wavenumber modes might allow substantial growth of vortex structures and a rapid enhancement of the plasma kinetic energy. While it is not obvious that KH modes have flows and structures which allow the driving of hybrid shear flow ballooning modes, we will show the results of linear analysis and nonlinear computer simulations which indicate that this coupling can occur. In the linear stage, the system develops a KH-like mode which generates a vortex. In the nonlinear stage, this vortex drives radial flows which disturb the initial equilibrium pressure. The pressure perturbations are unstable with respect to the RT instability and initiate cell-like flows which constructively add to the initial vortex. This nonlinear interaction results in the growth of a KH-RT hybrid mode, which starts from large amplitude with a spatial scale that is defined by the nonlinear KH-like vortex. It will be shown that the

¹On leave from the P. N. Lebedev Physics Institute, Russian Academy of Science, Moscow.

Copyright 1997 by the American Geophysical Union.

Paper number 97JA00386.
0148-0227/97/97JA-00386\$09.00

hybrid instability can grow very rapidly in the equatorial magnetosphere, with e -folding times of the order of tens of seconds.

In this study, we consider a simplified nonlinear model of shear flow and hybrid instabilities in the equatorial plane of the plasma sheet. Our major objective is to show that hybrid modes can grow and to explain the coupling that exists between shear flow and pressure gradient modes. We assume that initially a constant earthward pressure gradient provides a tailward force which is in equilibrium with an earthward "effective gravitational force," which models the effect of magnetic field line curvature. The computer model shows that the instability evolves as a two stage process. The initial vortex formation is very much like that found for the KH instability, though the vortex evolves somewhat more rapidly when pressure gradients are present. Following this initial stage, the system can develop strong radial flows and "billows" like those found in Rayleigh-Taylor or ballooning modes. In this way, the shear flow instability can work as a trigger for a pressure gradient energy release.

We compare the effect of unidirectional and bidirectional shear flows on the excitation and growth of convective cells. The former can provide stronger excitation but faster saturation, because of azimuthal motion of vortices. The latter can generate much larger immobile convective cells.

2. Theoretical Model

2.1. Basic Equations

We adopt a magnetohydrodynamic (MHD) set of equations that will be used to model plasma in the equatorial region of the inner edge of the plasma sheet:

$$\frac{\partial \mathbf{B}}{\partial t} - \nabla \times (\mathbf{V} \times \mathbf{B}) = 0, \quad (1)$$

$$\rho \frac{\partial \mathbf{V}}{\partial t} + \rho (\mathbf{V} \cdot \nabla) \mathbf{V} + \nabla (P + \frac{B^2}{8\pi}) - \frac{1}{4\pi} (\mathbf{B} \cdot \nabla) \mathbf{B} = 0, \quad (2)$$

$$\frac{\partial \rho}{\partial t} + \nabla \cdot (\rho \mathbf{V}) = 0, \quad (3)$$

$$\frac{d}{dt} \left(\frac{P}{\rho^\gamma} \right) = 0. \quad (4)$$

In these equations, \mathbf{B} is the magnetic field, \mathbf{V} is the fluid velocity, ρ is the plasma density, P is the thermodynamic pressure, and γ is the adiabatic constant. We neglect the effect of magnetic field line tying in the ionosphere and concentrate on a local analysis of the instability in the equatorial region of the plasma sheet. We shall develop a model which assumes that magnetic field lines are stretched slightly tailward and consider the case where the radius of meridional magnetic field line curvature is much smaller than the radius of azimuthal curvature. In this study, we choose a fluid treatment of the problem, neglecting kinetic or finite Larmor radius effects, and have assumed that resistivity is negligible. These limitations will be discussed in section 4.

In the equatorial plane, there are two forces produced by magnetic field line curvature that act on plasma in the radial direction: the particle inertial force $\rho V_z^2/R$ directed tailward and the magnetic curvature force $-B_z^2/4\pi R$ acting earthward, where z is the direction of the ambient magnetic field and R is the radius of the magnetic field line curvature in the meridional plane. For simplicity, in this study we assume that the difference between these two forces produces an effective centripetal acceleration \mathbf{g} in the earthward direction, which is considered to be constant in the interaction region. This assumption allows us to incorporate a Cartesian geometry, in which the x axis is directed earthward, the y axis is in the dawn-dusk direction, and the z axis is in the ambient magnetic field direction. This geometry is demonstrated in Figure 1. We suppose that the shear flow is directed in the azimuthal direction, $V_y = V_0(x)$. In equilibrium, the plasma density, pressure, magnetic field, and shear flow velocity are considered to be functions of x only. These assumptions are similar to those made in other papers devoted to a local analysis of shear flow processes [Viñas and Madden, 1986; Miura and Pritchett, 1982]. The dynamics of the shear flow in a plasma with a pressure gradient can then be described using the two-dimensional form of MHD in (1)-(4) with (2) replaced by

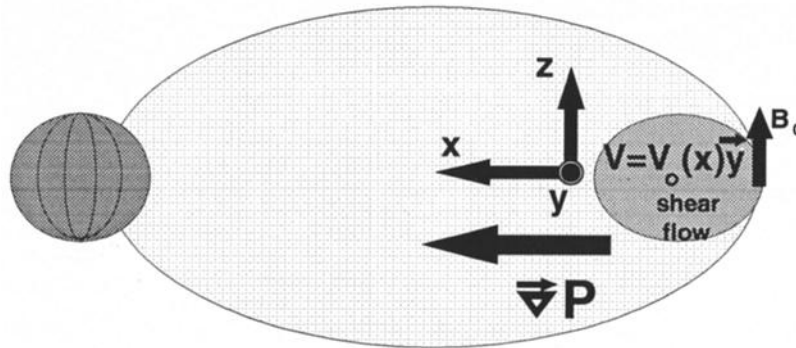


Figure 1. The geometry of the inner plasma sheet: a shear flow is embedded in a region of pressure gradient and stretched magnetic field lines.

$$e \frac{\partial \mathbf{V}}{\partial t} + e(\mathbf{V} \cdot \nabla_{\perp})\mathbf{V} + \nabla_{\perp}(P + \frac{B^2}{8\pi}) - e\mathbf{g} = 0, \quad (5)$$

where ∇_{\perp} stands for the gradient in the equatorial plane.

Our equilibrium is defined as the balance between the effective acceleration and pressure force,

$$\rho_0 g = \frac{\partial}{\partial x}(P_0 + \frac{B_0^2}{8\pi}). \quad (6)$$

We consider the stability of this equilibrium with respect to a small perturbation $e^{i(ky - \omega t)}$. Assuming that the half width of the shear flow δ is much smaller than the pressure gradient spatial scale L , one can reduce the system of MHD equations above to an equation for the radial component of the flow velocity V_x ,

$$V_x'' = k^2 V_x (1 - \frac{V_0''}{k(\omega - kV_0)} - \frac{W}{(\omega - kV_0)^2}), \quad (7)$$

where

$$W = -\frac{g\rho_0'}{\rho_0} - \frac{g^2}{V_f^2} \quad (8)$$

is the analog of the Brunt-Väisälä frequency [Pedlosky, 1987], $\omega - kV_0(x)$ is a Doppler-shifted wave frequency, $V_f^2 = C_s^2 + V_a^2$ is the square of the fast mode velocity, $V_0(x)$ is the shear flow velocity, and the prime symbol stands for the derivative with respect to x . C_s and V_a are acoustic and Alfvén velocities, respectively.

2.2. Qualitative Analysis of the Hybrid Mode Instability

Equation (7) describes velocity perturbations that arise due to a pressure gradient (W) and a shear flow (V_0). Depending on the sign of W , the pressure gradi-

ent may be stable ($W > 0$) or unstable ($W < 0$). In the case where the thermal pressure is a function of radial distance, whereas the density and magnetic field are uniform in the equilibrium state, W is always negative and therefore the RT growth rate γ_{RT} is positive: $\gamma_{RT} \sim (-W)^{1/2} \sim V_f/L$ for $k \gtrsim 1/L$, where L is the scale of the pressure gradient. The KH instability also has a positive growth rate, $\gamma_{KH} \sim V_0/\delta$, for wave numbers $k \sim 1/\delta$. Now we demonstrate that these two processes interact in a constructive way, thereby increasing the growth rates of both instabilities and generating a new hybrid mode. This hybrid mode has both RT-cell and vortical (KH) components and allows for energy exchange between them.

The physical processes responsible for the coupling can be described as follows (Figure 2). Let us assume that $\rho_0(x)$ and $g(x)$ are constant and that the gradient of plasma pressure is caused by a temperature gradient in the region where the shear flow exists. We also assume that $V_0/\delta \gg V_f/L$, so that the KH instability has the faster growth rate. This means that the instability is initiated as a pure KH instability which generates a vortex as follows: Suppose that a small perturbation of the radial component of the velocity appears in the shear flow. This involves motion of plasma from a region of higher velocity V_{y1} to a region of lower velocity V_{y2} (perpendicular to the ambient flow) and leads to a reduction of the velocity in the y direction. However, if the plasma is incompressible, this reduction of V_y should be compensated by a gain in the x component in order to maintain the velocity divergence free. Therefore the flow deviates from its initial direction. This initiates a shear flow vortex shown in the center of Figure 2. Now let us assume that this KH vortex evolves in a plasma with a temperature gradient and therefore involves a transfer of plasma energy along stream lines. Let us consider the evolution of the plasma pressure and effective gravity in association with plasma motion along

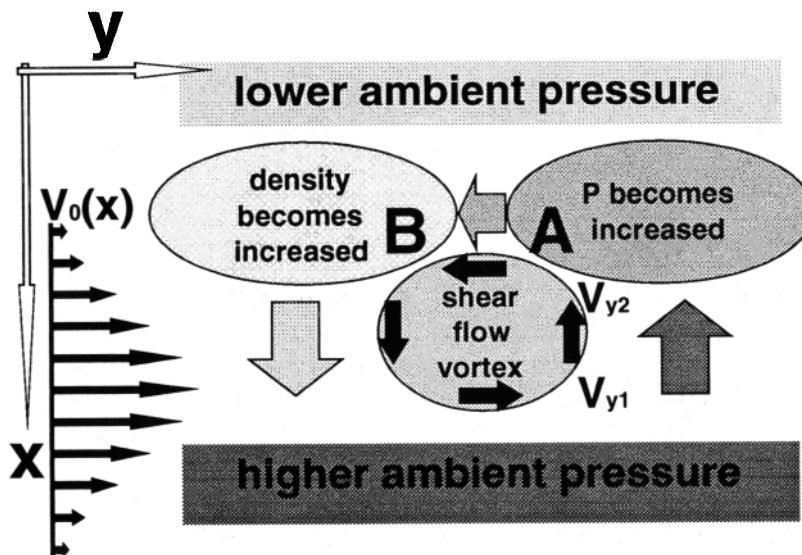


Figure 2. A schematic showing the interaction of a shear flow vortex with a pressure gradient cell. A Gaussian-shaped shear flow is assumed.

flow streamlines. In Figure 2, the radial flux into cell A, initiated by the flow from region V_{y1} to region V_{y2} , is opposite the plasma pressure gradient and involves motion of plasma from a hotter region to a colder region. The colder region allows the hotter region to expand, so that the plasma pressure grows in cell A. The increased pressure in cell A initiates a plasma flow in the y direction, which contributes to the vortex component and is associated with plasma motion into cell B, providing for a growth of the density in the cell B. As a result, the radial component of the effective force $\rho g - \nabla P$ deviates from its equilibrium value and is directed out of cell B along the KH vortex streamlines. The resulting acceleration provides additional growth of the KH vortex. Therefore the RT mode accelerates the shear flow vortex and provides a constructive interaction between these two modes.

2.3. Linear Theory of the Hybrid Instability

The solution to (7) was found numerically using a spectral method (see appendix). The growth rate for pure Kelvin-Helmholtz, hybrid (KH+RT), and noninteracting RT modes is shown in Figure 3. A Gaussian profile for the shear flow in the radial x direction was chosen in the following form: $V_y(x)/V_0 = \exp(-(x - x_0)^2/\delta^2)$. The Brunt-Väisälä frequency for this case corresponds to $W\delta^2/V_0^2 = -0.01$. The hybrid mode shown in Figure 3 is a result of the coupling of the main RT and KH modes. This mode behaves as a pure RT mode when k approaches 0. When k is extremely small, γ goes to 0 (not shown in Figure 3). Figure 3 also shows that the hybrid mode is suppressed for $k \geq 2/\delta$. The KH vortex may develop only for $k \lesssim 2/\delta$, and the hybrid vortex spectra is also limited to these wavenumbers. At the same time, the linear analysis reveals an existence of noninteracting RT modes which develop independently in the system. As demonstrated in Figure 3, only noninteracting RT

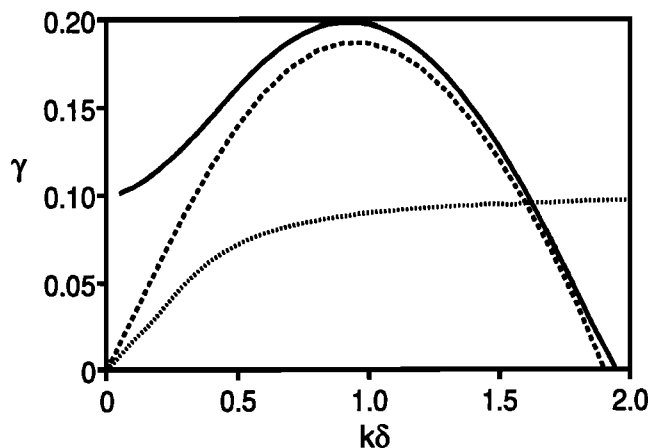


Figure 3. Growth rate $\gamma = \text{Im}(\omega)\delta/V_0$ of hybrid mode (solid line), KH instability (dashed line), and noninteracting RT mode (dotted line) as a function of $k\delta$. The growth rates for hybrid and noninteracting modes are computed for $W(\delta/V_0)^2 = -0.01$.

modes may develop in the system for $k \gtrsim 2/\delta$, whereas the hybrid mode is suppressed.

The formation of both interacting and noninteracting modes is further explained in Figure 4. In Figure 4, the solid arrows show the direction of plasma motion due to the KH vortex, whereas the empty arrows indicate plasma flow within RT cells. An initial perturbation, which develops into a vortex, is in phase with a large-scale ($k_x \sim 1/L$) RT cell in Figure 4a. In this case, the RT mode interacts with the vortex, and coupling occurs. The growth rate of this mode corresponds to the solid line in Figure 3. Now let us consider the RT mode with the radial wavenumber $k_x \sim 2/L$. This RT mode is shown in Figure 4b and consists of two RT cells in the radial direction. It equally enhances (in the bottom part) and suppresses (in the top part) the shear flow vortex, providing a net contribution of zero.

3. Numerical Results

The results of the linear analysis of the hybrid instability have been compared with numerical solutions to the full set of MHD equations, (1) and (3)-(5). The two-dimensional simulations use an alternating direction implicit method [Finan and Killeen, 1981; Rankin et al., 1993b].

3.1. Vortex Evolution

In order to test the excitation and evolution of a hybrid vortex mode, a shear flow which is unstable to the KH instability was initiated in a plasma with a pressure gradient. The shear flow was chosen uniform in the y direction, with a Gaussian profile in the x direction of the form $V_y(x) = V_0 \exp(-(x - x_0)^2/\delta^2)$, where $V_0 = 100$ km/s, $\delta = 0.0425 \cdot R_E$ and x_0 is at the center of the simulation box in the radial direction. The length of our simulation box is $1.5 R_E$ in the radial direction and $2\pi/k$ (one wavelength) in the azimuthal direction. The mesh consists of 100 points in the azimuthal direction distributed uniformly and 120 points in the x direction. The resolution in the x direction varies from $0.009 R_E$ in the center of the box to $0.017 R_E$ at the boundaries. The initial plasma density and magnetic field were set as $\rho = 4.06 \cdot 10^{-24}$ g/cm³, and $B_0 = 0.0004$ G, respectively, with a uniform distribution in both the x and y directions. The Alfvén speed corresponds to $V_a = 560$ km/s, and the pressure corresponds to $P = 4.35$ nPa at x_0 and increases linearly along x (earthward in our model) with $\partial P/\partial x = 5.7$ nPa/ R_E .

First of all, we study the growth of a hybrid mode with $k = 0.7/\delta$. For wavelengths $k \sim 1/\delta$, the growth rate of the RT instability is small compared to the growth rate of the KH instability in our model, which means that the extraction of potential energy from the ambient plasma, and the formation of the RT cells, is slow. However, as predicted by the linear theory, the combination of a shear flow and a pressure gradient is expected to increase the growth of the vortex through the formation of a hybrid mode. The growth rate increase depends on the pressure gradient, and it is about

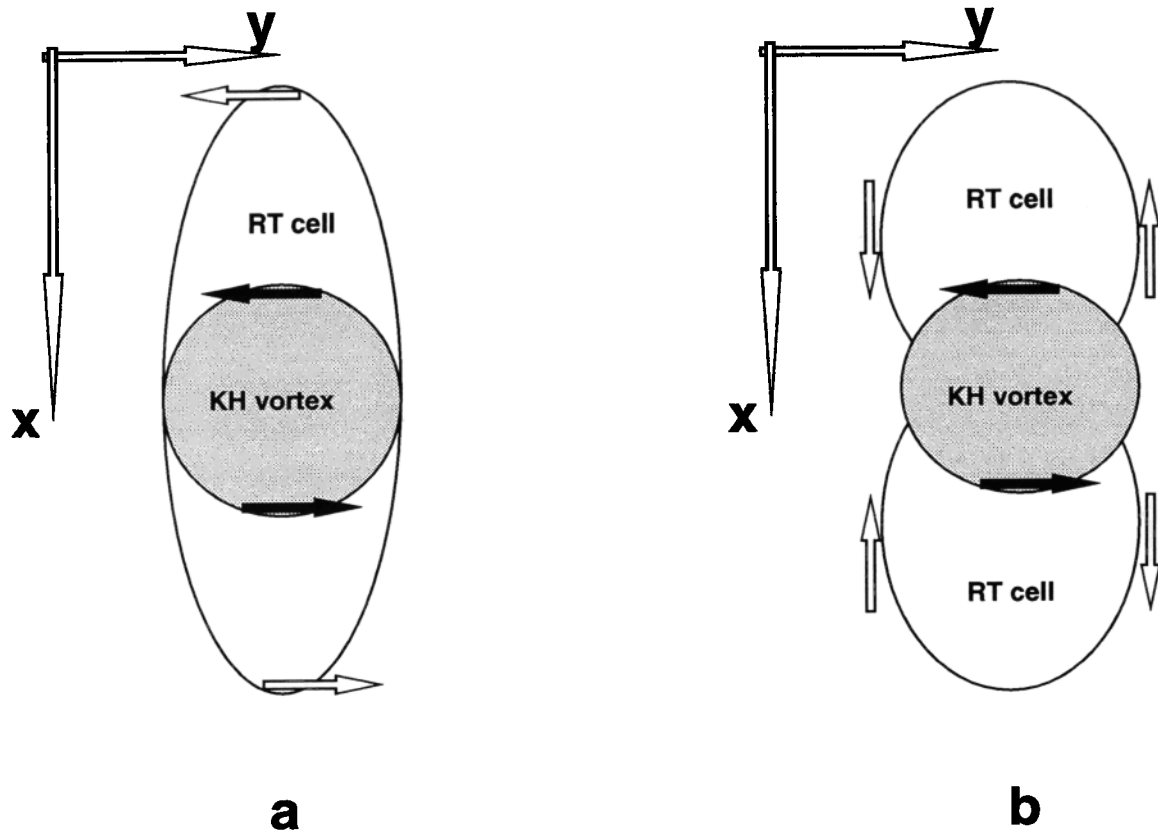


Figure 4. A model of the interaction of a shear flow vortex with RT modes of different radial scales: (a) $k_x \sim 1/L$ and (b) $k_x \sim 2/L$. Arrows show the direction of the plasma motion due to the KH vortex (solid arrows) and RT cells (empty arrows) formation

10% for the chosen parameters of the slightly unstable RT mode. The growth of the initial perturbation of the radial component of velocity is shown in Figure 5a for hybrid, KH, and RT modes, respectively. The velocity is normalized by V_a , whereas time is normalized by the Alfvén transit time $t_a = L/V_a = 17.1$ s. Figure 5b shows the growth of the kinetic energy normalized by the initial total kinetic energy of the shear flow:

$$\Delta\varepsilon = \frac{\int \rho V^2 dx dy}{\int \rho V_0^2 dx dy} - 1. \quad (9)$$

Let us consider the evolution of the hybrid mode in more detail. The growth of the instability shown in Figure 5 implies that there are two different stages of evolution with different physical processes involved. We can distinguish the following stages: the linear growth and saturation of the KH-like vortex and the nonlinear growth and saturation of the hybrid vortex. Snapshots of the z component of the vorticity $\Omega_z = (\nabla_{\perp} \times \mathbf{V})_z L/V_a$, for $t/t_a = 5, 7$, and 10 , respectively, which correspond to these stages of the instability evolution, are shown in Figure 6.

As seen in Figures 5 and 6, the first stage of the evolution, $t/t_a \leq 6$, corresponds to the linear formation of a KH-like vortex. For our choice of parameters, γ_{KH} is almost 2 times larger than γ_{RT} . Hence the formation of a hybrid vortex is initially similar to the formation

of a shear flow vortex with no pressure gradient in the plasma. However, the growth rate of the hybrid mode is slightly greater than for the KH mode because of the positive interaction of the KH instability with a large-scale RT cell. At this stage of the vortex formation, the kinetic energy of the initial shear flow is transformed into vortex kinetic energy, but the total kinetic energy does not increase, which corresponds to $\Delta\varepsilon \sim 0$ (see Figure 5b). The insignificant trend downward from zero is caused by the small numerical viscous damping which is required to stabilize the numerical scheme.

The first linear stage of the evolution is complete by the time $t/t_a \sim 6$. The KH instability is then nonlinearly saturated because of the shear flow expansion in the radial direction (see Figure 6). At this stage, the hybrid vortex experiences a transition from KH-like to azimuthally moving RT-like. This transition is evident on comparing the contour panels of Figure 6, where it can be seen that billows are starting to form in the hybrid mode evolution. Figure 7 demonstrates this transition for the main plasma parameters characterizing the instability: the radial component of the velocity, density, and plasma pressure. The significant changes observed in the density and pressure indicate the beginning of the nonlinear KH-RT interaction. The KH vortex defines the spatial shape of the cell and sets up a large perturbation from which further growth of the RT-like instability within the cell can occur. This

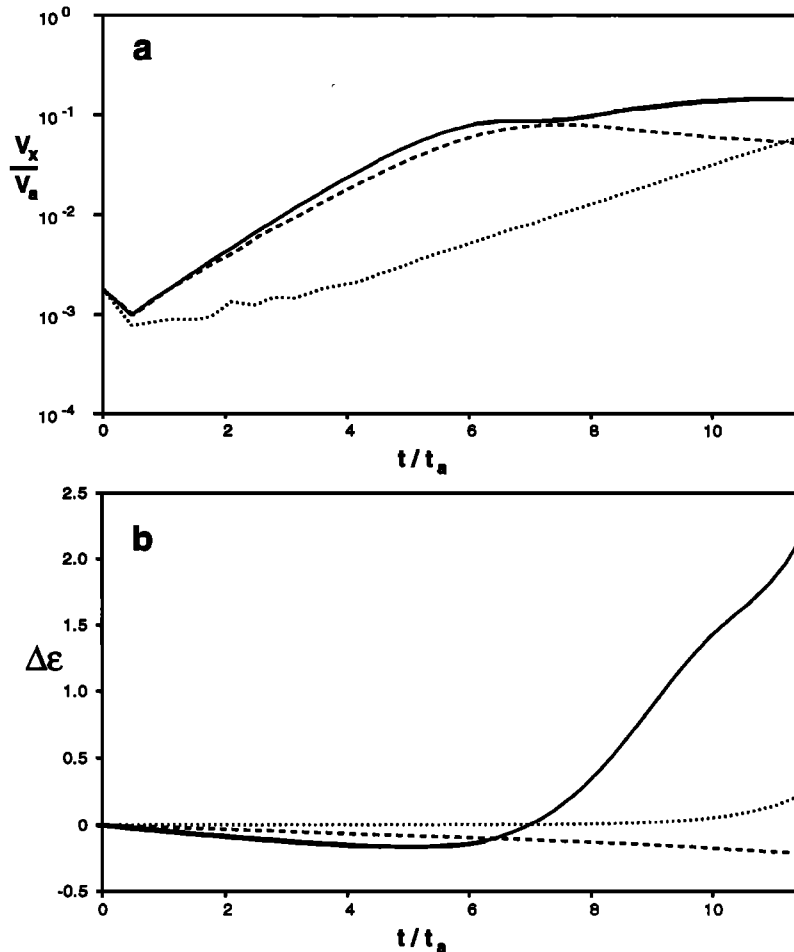


Figure 5. Growth of (a) amplitude of the radial velocity V_x and (b) the integrated kinetic energy of the hybrid mode (solid line), KH mode (dashed line), and RT mode (dotted line), respectively. Parameters are given in the text.

provides a constructive interaction between the KH and RT modes and also explains why this transition stage is comparatively short, $\Delta t/t_a \sim 1$. As seen in Figure 7, a new interchange cell is formed within the shear flow which has a radial scale comparable to the width of the shear flow. The growth rate of the RT instability of this cell is smaller than the growth rate of the large-scale cell which was associated with the linear stage of the evolution.

When the transition stage is over, the developed hybrid vortex continues to grow, as can be seen from an inspection of Figures 5 and 6 for $t/t_a \geq 7$. At this stage, the growth is slower than for the first stage and is comparable to the RT-instability growth rate of a cell which has the radial scale of the shear flow. This growth is accompanied by an extraction of the ambient potential energy and its transformation into kinetic energy of the vortex. The total kinetic energy of the vortex grows far beyond the value of kinetic energy of the initial shear flow. For this example, the energy of the hybrid vortex is approximately 3 times larger than the energy of the initial shear flow by the time $t/t_a \sim 11$. In contrast, the KH instability simulations indicate that a KH vortex with $k\delta \sim 1$ can only extract about one half of the total shear flow kinetic energy.

At this nonlinear stage, the instability modifies significantly the spatial distribution of the shear flow and pressure. By the time $t/t_a \sim 10$, further growth of the radial component of the velocity is restricted by the boundaries of the expanded flow. Thus, a portion of the vortex flow is then directed along the outer boundaries of the shear flow in order to provide momentum conservation. This initiates secondary flows in the direction opposite to the initial shear flow and leads to the azimuthally stretched and radially compressed flow structures shown in Figure 8. Figure 8 also displays a radial asymmetry, which is due to the radial gradient of the fast mode velocity V_f .

As mentioned above, at the nonlinear stage the hybrid vortex provides dramatic changes of the plasma pressure which characterizes the potential energy distribution in the plasma. This redistribution of plasma pressure in the equatorial plane of the magnetotail is expected to cause a redistribution of magnetic field aligned currents thus providing further dynamics in the magnetosphere-ionosphere coupling.

Saturation of the nonlinear hybrid vortex occurs when the vortex size in the radial x direction becomes comparable to the width of the zeroth order expanded shear flow, which is then stable with respect to the KH insta-

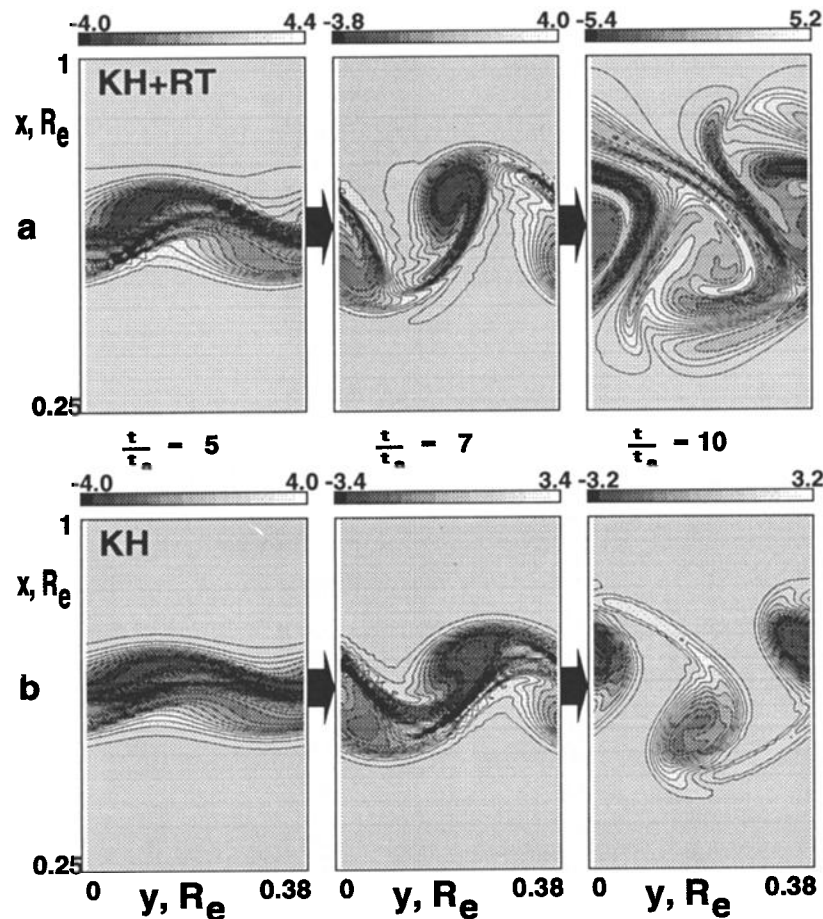


Figure 6. Time slices of the vorticity as obtained from the computer simulations for the (a) hybrid mode and (b) KH instability for $t/t_a = 5, 7,$ and 10 .

bility. Nevertheless, new large-amplitude perturbations of the radial component of the velocity appear in the secondary reversed flows discussed above. The resulting vortices can be clearly seen at the boundaries of the shear flow in Figure 8. These vortices provide for a further interaction with interchange cells. Figure 9 demonstrates the radial distribution and time evolution of the radial kinetic energy $\langle V_x^2 \rangle = k/(2\pi) \int_0^{2\pi/k} V_x^2 dy$. The growth of the radial component of the velocity within the shear flow terminates at the time $t/t_a \sim 10$, whereas the perturbations which appear at the edge of the shear flow then start growing. This growth provides a further extraction of the potential energy of the plasma and a corresponding growth of the kinetic energy of the newly generated vortex structures. This stage is seen in Figure 5b as kinetic energy growth which starts at $t/t_a \sim 11$. The latest nonlinear stage is similar to the edge effects of the RT-KH interaction described in the fusion literature [Drake *et al.*, 1992; Finn *et al.*, 1992; Finn, 1993].

3.2. Wavelength Dependence

The azimuthal size of the vortex is a parameter in our model and is defined by the wavenumber k of the initial perturbation. If the perturbation has a short wavelength ($k \geq 2/\delta$), the hybrid mode is stable (see

Figure 3), and only RT modes with larger wavenumbers in the radial direction (see Figure 4b) are unstable. The results of simulations for the mode $k\delta = 1.8$ are presented in Figure 10a. In this case, the shear flow, which is stable with respect to the KH instability, divides the pressure gradient area into two parts, and the noninterchange RT mode predicted by the theory to be unstable (see Figure 4b) grows above and below the shear flow and stabilizes in the vicinity of the flow.

In the other extreme case of large wavelengths, the hybrid mode is predicted to be unstable, but the interchange component dominates. Thus the evolution of the hybrid vortex is defined by the RT instability, which evolves slower but leads to a strong deformation of the shear flow within the cell. The hybrid vortex takes the shape of a large-scale fold, as shown in Figure 10b for $k = 0.2/\delta$.

3.3. Bidirectional (Antisymmetric) Flow

In the previous sections, we considered a unidirectional Gaussian shear flow. We found that the hybrid mode extracts potential energy from the ambient plasma, but the extension of the vortex in the radial direction is restricted by the boundaries of the initial shear flow. This restriction of the radial vortex expansion originates from the azimuthal motion of vortices

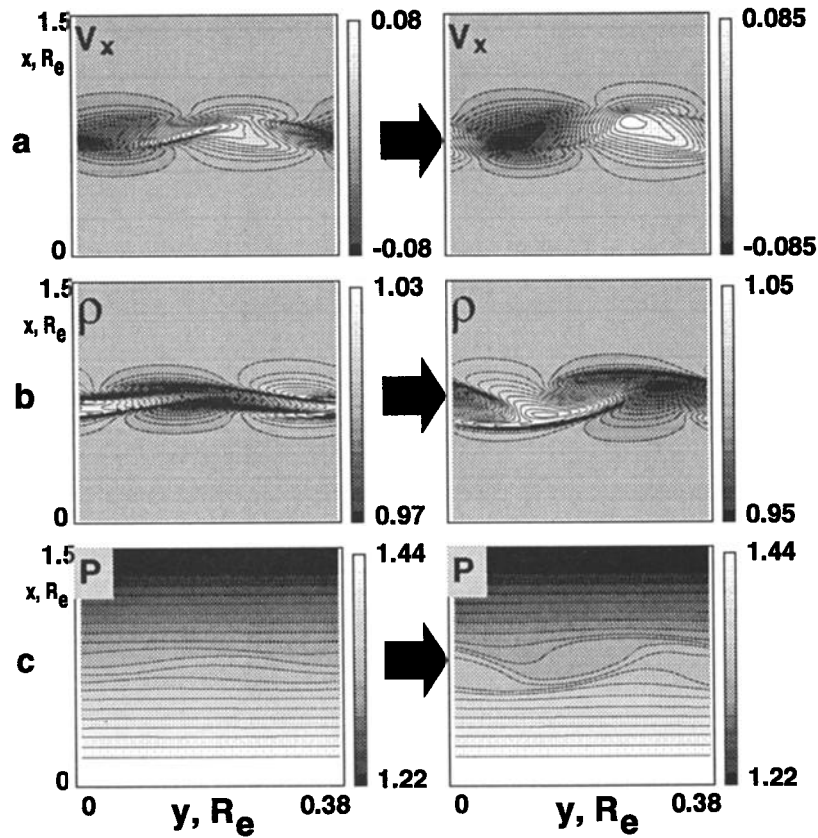


Figure 7. Contour plots of (a) V_x , (b) density, and (c) plasma pressure for $t/t_a = 6$ and 7 , respectively, illustrating the transformation of the hybrid eigenmode from KH-like to RT-like.

and interchange cells. Outside of the region of the shear flow, interchange cells no longer move in the azimuthal y direction, and the original hybrid vortex slides by the interchange cells without interaction. This process may be illustrated using Figure 2 if we imagine that a vortex

moves with the shear flow in the y direction. Then it provides a constructive interaction with an interchange cell for a half period, when it is in between sections A and B, whereas the interaction is destructive when the vortex moves farther to the right side of section A.

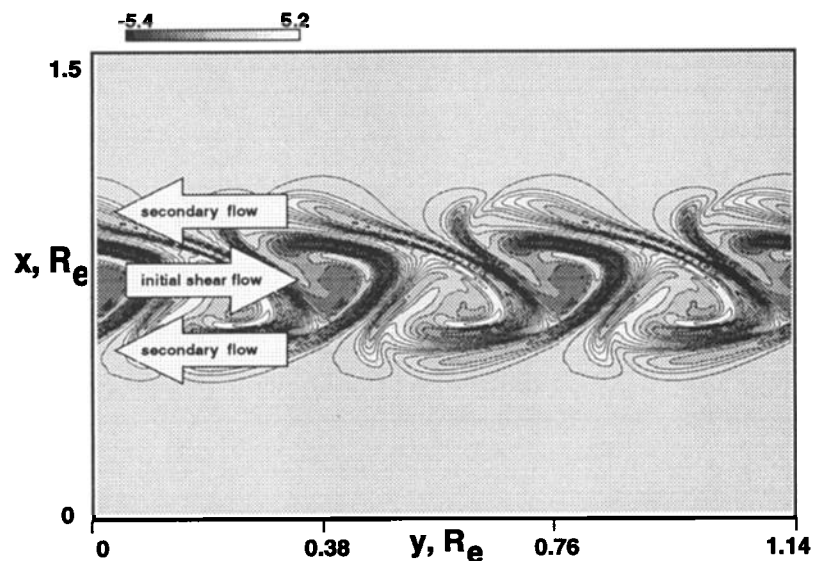


Figure 8. The vorticity of the hybrid mode for $t/t_a = 10$, demonstrating the generation of secondary shear flows which elongate the vortices in the direction that is opposite the initial shear flow. Three cells in the azimuthal direction are combined in order to show a whole vortex structure.

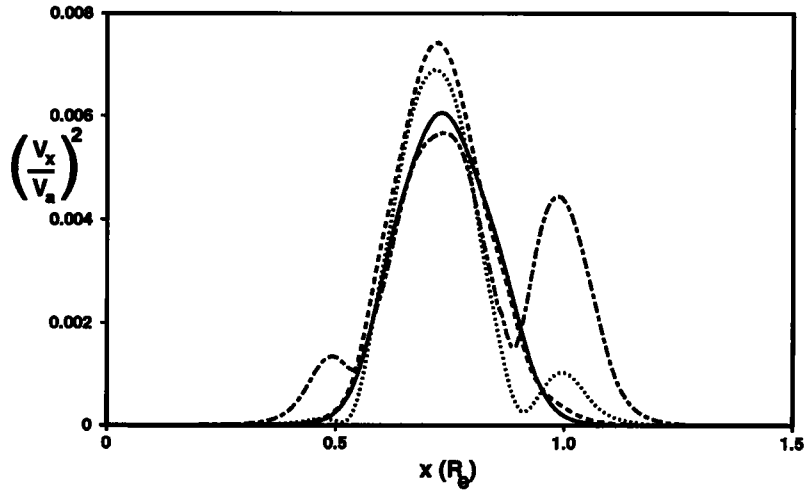


Figure 9. Radial distribution of the integrated radial kinetic energy $\langle V_x^2 \rangle$ at time $t/t_a = 8.8$ (solid line), 9.8 (dashed line), 10.7 (dotted line), and 11.6 (dashed-dotted line).

Therefore the motion of the hybrid vortex may turn off its interaction with a larger-scale interchange cell. This interaction may be restored if the vortex does not move with respect to the ambient plasma. These types of vortices are produced by the KH instability of a bidirectional (antisymmetric in the radial direction) shear flow.

We consider the evolution of a hybrid vortex for a shear flow defined by $V_y(x) = 2.5 V_0 \tanh((x - x_0)/\delta)/\cosh^2((x - x_0)/\delta)$ with $V_0 = 50$ km/s and $\delta = 0.0425 \cdot R_E$. Other parameters remain the same as in previous examples. The time slices of the vorticity of the hybrid mode are shown in Figure 11 for $k = 1/\delta$ (Figure 11a) and $k = 0.5/\delta$ (Figure 11b). The growth of the mode $k = 0.5/\delta$ is slower during the initial linear stage, but in the nonlinear stage it grows faster and reaches a greater amplitude than for the mode with

$k = 1/\delta$. Also, for the $k = 0.5/\delta$ mode, the vortex expands into the broad area beyond the shear flow, whereas shorter wavelength modes are still bounded by the shear flow radial extent. These two cases may be explained by the difference that exists between the saturated state of the KH vortices. The mode with the shorter wavelength is immersed in the shear flow. It can interact only with moving interchange cells and therefore cannot leave the region of the shear flow. Finally, this mode saturates at the edges of the shear flow. This saturation is similar to the saturation of the hybrid mode which develops from the unidirectional flow as discussed in section 3.1. On the other hand, if larger-scale perturbations develop in the bidirectional flow, they evolve into vortical structures that have two characteristic lengths: one scale involves small vortical structures within the flow and the second scale involves

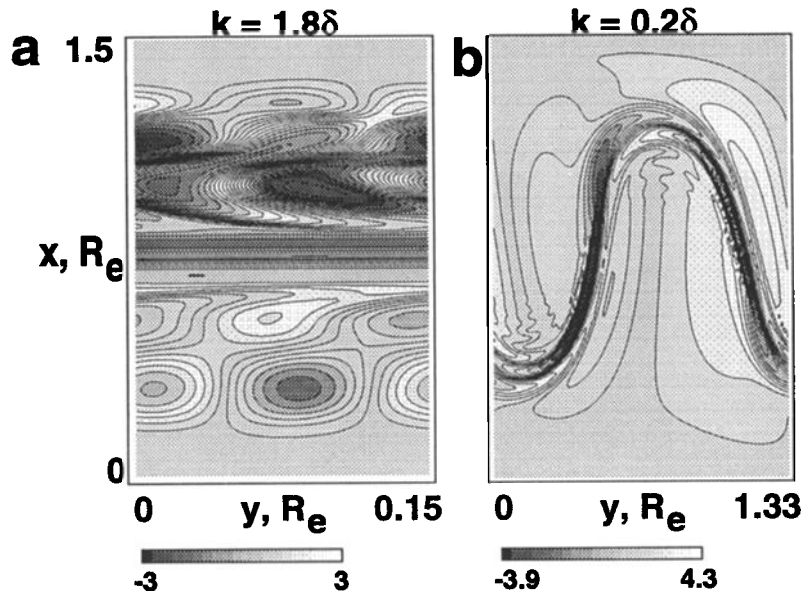


Figure 10. The vorticity for (a) small ($k = 1.8/\delta$) and (b) large ($k = 0.2/\delta$) wavelength perturbations.

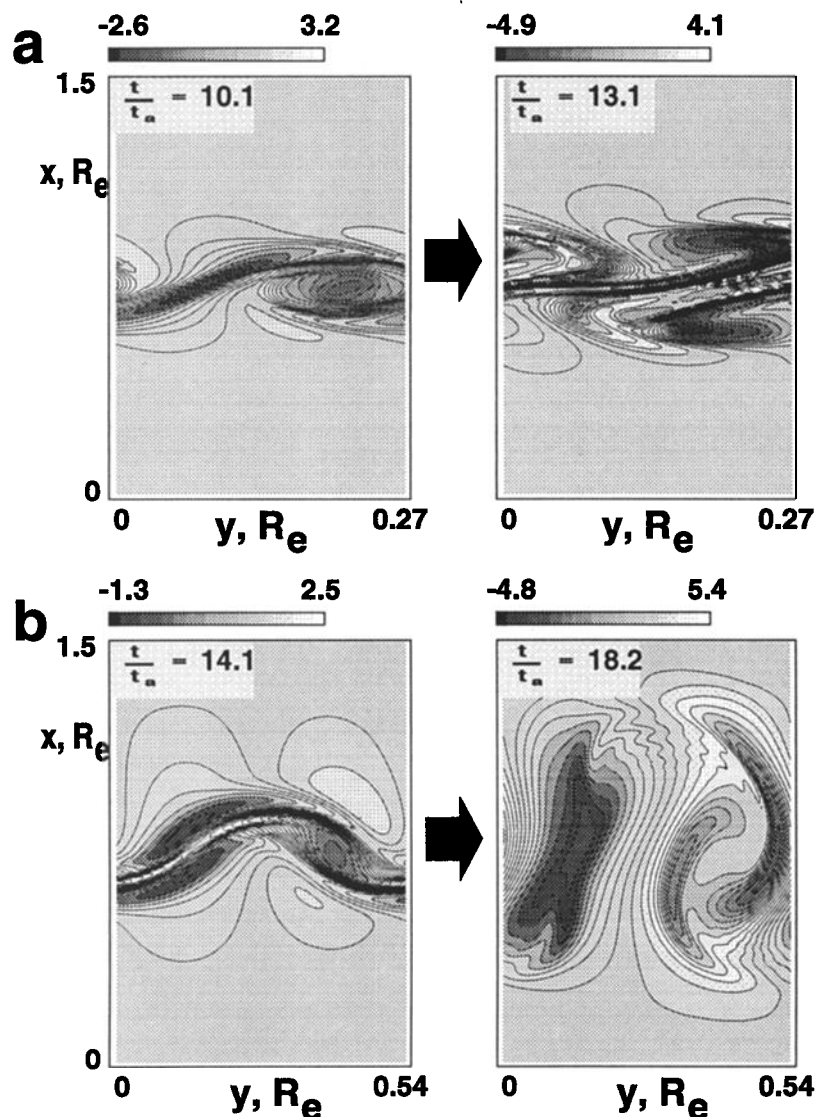


Figure 11. Time slices of the vorticity obtained from the computer simulations for the hybrid mode driven by a bidirectional shear flow with (a) $k = 1/\delta$ ($t/t_a = 10.1$ and 13.1) and (b) $k = 0.5/\delta$ ($t/t_a = 14.1$ and 18.2).

a larger distortion of the shear flow itself. This large-scale distortion can easily interact with a large-scale interchange cell in the plasma gradient region. The resulting hybrid vortex expands in the radial direction finally destroying the initial shear flow and significantly extending the scale of the immersed vortical structures.

4. Discussion

Our computer simulation of the interaction of the KH instability with a pressure gradient has revealed a multistage evolution of the vortex structure. Initially, the vortex generation is qualitatively similar to the pure KH instability. Quantitatively, the vortex develops faster in the presence of the pressure gradient because of the constructive interaction of a shear flow vortex with a larger scale RT cell in the radial direction. Later in time, the hybrid vortex extracts potential energy from the ambient plasma, providing further growth of the kinetic energy of the vortex. This scenario suggests an expla-

nation for observations, indicating that only vortices in the late evening and midnight sectors, where the pressure gradient is large, may develop in association with vigorous surges, whereas vortices in the earlier evening sector appear and vanish without further evolution.

It follows from the simulations that perturbations with wavenumbers $k \sim 0.5/\delta$ imposed onto a bidirectional flow can evolve into large-amplitude surge-like structures which can destroy the original shear flow and expand over a wide region during a characteristic time of tens of seconds. Similar behavior was experimentally confirmed by *Steen and Collis* [1988] during observations of the westward traveling surge.

The theory and numerical results presented above are a simplified model of complicated processes in the inner plasma sheet. A primary goal of this model was to consider a situation in which an unstable shear flow appears on the background of a pressure gradient which is initially in equilibrium with a force that is imposed by the curvature of stretched magnetic field lines. This

force acts on the plasma in the earthward direction and is assumed to be in the simple form $\rho \cdot \mathbf{g}$, where \mathbf{g} stands for a centripetal acceleration of the particles as a result of both magnetic curvature and particle inertia. Generally, magnetic curvature may vary in time as a result of the temporal evolution of magnetotail currents or through currents produced by the instability itself. Particle inertia may evolve in time as well, because of an acceleration along magnetic field lines and/or growth or decay of the parallel energy of the particles. In this model, we have neglected these effects.

In this study, we have adopted a fluid model that neglects kinetic or finite Larmor radius effects. This means that our model is valid for describing the evolution of structures with a spatial extension larger than the Larmor radius. For the sample shear flow and chosen density, the ion Larmor radius is smaller than the scale size of the vortices. However, if the initial shear flow is thinner or if fine structure of vortices is to be studied, ultimately, kinetic effects should be taken into account. Kinetic and fluid-kinetic hybrid treatments have been presented by *Ganguli et al.* [1988], *Thomas and Winske* [1993], and *Huba* [1996]. These studies revealed the importance of small-scale effects and their influence on the growth rate and frequency of the shear flow instability. Also, the kinetic effects may be responsible for an asymmetry of the instability with respect to the center of the flow [*Thomas*, 1995; *Huba*, 1996]. All of these effects may be valid for the auroral arc fine structure dynamics and can be considered as an important direction toward a comprehensive auroral arc model.

The other problem to be addressed is the importance of nonideal MHD terms which violate the frozen in flux condition. The importance of the Hall term for the KH instability evolution was described by *Huba* [1994] for spatial scales of the order of the Larmor radius. We neglected this effect by assuming that the width of the flow is larger than the Larmor radius. On the other hand, localized resistivity can initiate a large-scale tearing mode [see *Hesse and Birn*, 1994, and references therein]. This mode can be driven by magnetic curvature [*Sundaram and Fairfield*, 1995] and implies that in a resistive plasma, additional hybrid modes are expected. The interaction of the shear flow and vortices with these modes seems to be a significant problem which might be addressed in future investigations.

Our model is also significantly simplified because we have neglected field-aligned gradients of plasma parameters and have reduced our consideration to the equatorial plane of a symmetric magnetotail. Even though such an approach is limited in its ability to describe the full dynamics of auroral arc intensifications, it has allowed us to obtain a simple solution to the problem, which reveals some of the physical mechanisms that involve an acceleration and subsequent radial expansion of the vortex structure.

5. Conclusion

Theory and numerical simulations of the evolution of a shear flow embedded in a pressure gradient region

reveal a constructive interaction between the unstable shear flow mode (KH mode) and the Rayleigh-Taylor mode. In the linear stage of the instability, the KH vortex interacts with the main RT harmonic, which enhances the growth rate. When the KH-like vortex saturates, it experiences a short transition stage, at which point the vortex evolution changes from KH-like to RT-like. At the end of the transition stage, the hybrid vortex becomes a large-amplitude perturbation for the RT instability and experiences further growth.

In the nonlinear stage, the hybrid vortex defines the radial size of the interacting RT pressure gradient cell. This stage is characterized by an extraction of potential energy from the pressure gradient and its transformation into kinetic energy of the hybrid vortex. During this nonlinear stage, the vortex evolution depends on the azimuthal wavenumber as well as on the shape of the flow. A unidirectional flow generates vortices which move with respect to the ambient plasma, providing a constructive interaction of vortices and RT cells which move with the flow. The optimal wavenumber for this interaction corresponds to $k \sim 1/\delta$. The radial expansion of the vortex is restricted by the interaction of the vortex with the boundaries of the flow. This interaction saturates the hybrid vortex, but at the same time it modifies the flow and generates large-scale perturbations of the boundaries. This leads to a further interaction with a large-scale RT cell and a further extraction of potential energy from the pressure gradient.

A different evolution was obtained for a bidirectional shear flow with an instability wavenumber $k \sim 0.5/\delta$. The hybrid vortex takes the shape of a radially stretched fold which has no azimuthal motion. In the nonlinear stage, this vortex interacts with a large-scale RT cell and leads to a fast growth and radial expansion of the vortex.

Summarizing these results, we conclude that the suggested instability appears to be a valid candidate for providing shear flow vortex generation which is similar to the KH instability but which can also initiate the transformation of ambient potential energy into kinetic energy of vortices. This may lead to the formation of large-amplitude surges which can rapidly expand in the radial direction.

Appendix: Spectral Method for the Solution to (7)

Expanding the solution of (7) into a series of orthogonal functions

$$\Psi = \sum_{n=-N}^N C_n S_n, \quad (\text{A1})$$

where $S_n = e^{in\pi x/L}$, multiplying the equation by a complex conjugate value S_m^* , and integrating over the area $[-L; L]$, we end up with a set of linear algebraic equations for C_n in the form of an eigenvalue problem:

$$\sum_{n=-N}^N \left(-\frac{n^2 \pi^2}{L^2} \delta_{n-m} + \frac{1}{2L} (S_m^*, \alpha^2 S_n) \right) C_n = k^2 \sum_{n=-N}^N C_n \delta_{n-m}, \quad (\text{A2})$$

where

$$\langle S_m^*, \alpha^2 S_n \rangle = \int_{-L}^L \left(\frac{V_0'' k}{\omega - kV_0} + \frac{Wk^2}{(\omega - kV_0)^2} \right) \exp\left(\frac{i\pi x(n-m)}{L}\right) dx$$

is an operator defined by the physical parameters of the problem.

This equation is homogeneous and has a nontrivial solution if the determinant of its coefficients equals zero. This equation was solved to find out the eigenvalues ω . Then the eigenfunctions were restored for every given eigenvalue ω .

Acknowledgments. This research was supported by the Natural Sciences and Engineering Research Council of Canada (NSERC), the Canadian Space Agency, and the Russian Foundation for Basic Research under grant 96-02-16707-a.

The Editor thanks two referees for their assistance in evaluation this paper.

References

- Drake, J. F., J. M. Finn, P. Guzdar, V. Shapiro, V. Shevchenko, F. Waelbroeck, A. B. Hassam, C. S. Liu, and R. Sagdeev, Peeling of convection cells and the generation of sheared flow, *Phys. Fluids B*, **4**, 488, 1992.
- Elphinstone, R. D., et al., Observations in the vicinity of substorm onset: Implications for the substorm process, *J. Geophys. Res.*, **100**, 7937, 1995.
- Finn, J. M., Nonlinear interaction of Rayleigh-Taylor and shear instabilities, *Phys. Fluids B*, **5**, 415, 1993.
- Finn, J. M., J. F. Drake, and P. N. Guzdar, Instability of fluid vortices and generation of sheared flow, *Phys. Fluids B*, **4**, 2758, 1992.
- Finan, C. H., III, and J. Killeen, Solution of the time-dependent, three-dimensional resistive magnetohydrodynamic equations, *Comput. Phys. Commun.*, **24**, 441, 1981.
- Ganguli, G., Y. C. Lee, and P. J. Palmadesso, Kinetic theory for electrostatic waves due to transverse velocity shears, *Phys. Fluids*, **31**, 823, 1988.
- Hesse, M., and J. Birn, MHD modeling of magnetotail instability for localized resistivity, *J. Geophys. Res.*, **99**, 8565, 1994.
- Huba, J. D., Hall dynamics of the Kelvin-Helmholtz instability, *Phys. Rev. Lett.*, **72**, 2033, 1994.
- Huba, J. D., Finite Larmor radius magnetohydrodynamics of the Rayleigh-Taylor instability, *Phys. Plasmas*, **3**, 2523, 1996.
- Kidd, S. R., and G. Rostoker, Distribution of auroral surges in the evening sector, *J. Geophys. Res.*, **96**, 5697, 1991.
- Kistler, L. M., E. Möbius, W. Baumjohann, G. Paschmann, and D. C. Hamilton, Pressure changes in the plasma sheet during substorm injections, *J. Geophys. Res.*, **97**, 2973, 1992.
- Lyons, L. R., and J. C. Samson, Formation of the stable auroral arc that intensifies at substorm onset, *Geophys. Res. Lett.*, **19**, 2171, 1992.
- Miura, A., and P. L. Pritchett, Nonlocal stability analysis of the MHD Kelvin-Helmholtz instability in a compressible plasma, *J. Geophys. Res.*, **87**, 7431, 1982.
- Murphree, J. S., and M. L. Johnson, Clues to plasma processes based on Freja UV observations, *Adv. Space Res.*, **18**(8), 95, 1996.
- Ohtani, S.-I., and T. Tamao, Does the ballooning instability trigger substorms in the near-Earth magnetotail?, *J. Geophys. Res.*, **98**, 19369, 1993.
- Pedlosky, J., *Geophysical Fluid Dynamics*, 710 pp., Springer-Verlag, New York, 1987.
- Rankin, R., B. G. Harrold, J. C. Samson, and P. Frycz, The nonlinear evolution of field line resonances in the Earth's magnetosphere, *J. Geophys. Res.*, **98**, 5839, 1993a.
- Rankin, R., J. C. Samson, and P. Frycz, Simulations of driven field line resonances in the Earth's magnetosphere, *J. Geophys. Res.*, **98**, 21341, 1993b.
- Samson, J. C., L. R. Lyons, P. T. Newell, F. Creutzberg, and B. Xu, Proton aurora and substorm intensifications, *Geophys. Res. Lett.*, **19**, 2167, 1992.
- Samson, J. C., L. L. Cogger, and Q. Pao, Observations of field line resonances, auroral arcs, and auroral vortex structures, *J. Geophys. Res.*, **101**, 17373, 1996.
- Steen, Å., and P. N. Collis, High time-resolution imaging of auroral arc deformation at substorm onset, *Planet. Space Sci.*, **36**, 715, 1988.
- Sundaram, A. K., and D. H. Fairfield, Localized tearing modes in the magnetotail driven by curvature effects, *J. Geophys. Res.*, **100**, 3563, 1995.
- Tajima, T., W. Horton, P. J. Morrison, J. Schutkeker, T. Kamimura, K. Mima, and Y. Abe, Instabilities and vortex dynamics in shear flow of magnetized plasmas, *Phys. Fluids B*, **3**, 938, 1991.
- Thomas, V. A., Three-dimensional kinetic simulation of the Kelvin-Helmholtz instability, *J. Geophys. Res.*, **100**, 19429, 1995.
- Thomas, V. A., and D. Winske, Kinetic simulations of the Kelvin-Helmholtz instability at the magnetopause, *J. Geophys. Res.*, **98**, 11425, 1993.
- Viñas, A. F., and T. R. Madden, Shear flow-ballooning instability as a possible mechanism for hydromagnetic fluctuations, *J. Geophys. Res.*, **91**, 1519, 1986.
- P. Frycz, R. Rankin, J. C. Samson, V. T. Tikhonchuk, and I. Voronkov, Department of Physics, University of Alberta, Edmonton, Alberta, Canada, T6G 2J1. (e-mail: igor@space.ualberta.ca, rankin@space.ualberta.ca, samson@space.ualberta.ca)

(Received October 24, 1996; revised January 29, 1997; accepted February 6, 1997.)